Tailoring Correlations of the Local Density of States in Disordered Photonic Materials

F. Riboli,[1,2,3,*] F. Uccheddu,[4] G. Monaco,[1] N. Caselli,[3,5,6] F. Intonti,[3,5] M. Gurioli,[3,5] and S. E. Skipetrov[7,8,†]
[1]Department of Physics, University of Trento, via Sommarive 14, 38050 Povo (TN), Italy
[2]Istituto Nazionale di Ottica, CNR, via Nello Carrara 1, 50019 Sesto Fiorentino, Italy
[3]European Laboratory for Nonlinear Spectroscopy, via Nello Carrara 1, 50019 Sesto Fiorentino (FI), Italy
[4]Department of Industrial Engineering, University of Florence, via Santa Marta 5, 50139 Firenze, Italy
[5]Department of Physics, University of Florence, Via G. Sansone 1, 50019 Sesto Fiorentino (FI), Italy
[6]Instituto de Ciencia de Materiales de Madrid, CSIC, Calle Sor Juana Ins de la Cruz, 3, Madrid, Spain
[7]Université Grenoble Alpes, LPMMC, F-38000 Grenoble, France
[8]CNRS, LPMMC, F-38000 Grenoble, France
(Received 6 September 2016; published 25 July 2017)

We present experimental evidence for the different mechanisms driving the fluctuations of the local density of states (LDOS) in disordered photonic systems. We establish a clear link between the microscopic structure of the material and the frequency correlation function of LDOS accessed by a near-field hyperspectral imaging technique. We show, in particular, that short- and long-range frequency correlations of LDOS are controlled by different physical processes (multiple or single scattering processes, respectively) that can be—to some extent—manipulated independently. We also demonstrate that the single scattering contribution to LDOS fluctuations is sensitive to subwavelength features of the material and, in particular, to the correlation length of its dielectric function. Our work paves a way towards complete control of statistical properties of disordered photonic systems, allowing for designing materials with predefined correlations of LDOS.

DOI: 10.1103/PhysRevLett.119.043902

After more than a hundred years of intense research on light propagation in random media, we are starting to realize that disorder is not only a nuisance for imaging and telecommunications but that it can be exploited to design new functional materials outperforming "clean" systems in a number of applications [1–8]. However, designing an efficient disordered photonic material requires controlling the statistics of its optical properties. Such a control has already been achieved, to a large extent, for transport properties governing propagation of light (scattering and transport mean free paths, diffusion coefficient, etc. [9]) but remains only partial for the properties relevant for the emission of light. The latter is a complicated process [10] but in many situations its efficiency, as well as absorption efficiency and many other types of light-matter interaction, depend on the local density of states (LDOS) at the source position [11]. LDOS $\rho(\mathbf{r},\nu)$ is simply a number of optical states (modes) at a point $\mathbf{r}$ and at a frequency ν, per unit volume and unit frequency band. In a disordered material, LDOS fluctuates in space and with the frequency of light [9] as demonstrated in recent experiments [12–15]. Fluctuations of LDOS at the source position lead to fluctuations in the decay rate of spontaneous emission [11] and produce long-range spatial correlations of emitted intensity in the far field [16].

Here we probe LDOS statistics using the near-field hyperspectral imaging technique [17]. Our experiments probe photoluminescence (PL) of InAs quantum dots (QDs) embedded in dielectric (GaAs) planar waveguides. Disorder is realized by perforating the waveguides with randomly distributed circular holes [17,18]. The QDs are excited through a dielectric tip of a near-field optical microscope (SNOM) with a low-power diode laser. PL of QDs is collected through the same tip [see Fig. 1(b)]. The measured PL intensity $I_{\mathrm{PL}}(\mathbf{r},\nu)$ is recorded every 200 nm on a square spatial grid. As we show in Fig. 1(a), $I_{\mathrm{PL}}(\mathbf{r},\nu)$ exhibits strong fluctuations with both the position of the SNOM tip $\mathbf{r}=(x,y)$ [Fig. 1(c)] and frequency ν [Fig. 1(d)]. A typical set of data for one sample comprises a region of interest of 18×18 μm, centered in the middle of the sample, far from the boundaries. For each position of the SNOM tip we collect PL signal between 218 and 260 THz with a frequency resolution of 0.1 THz. The fluctuations of PL intensity are characterized by an intensity correlation matrix

$$C_{\mathrm{PL}}(\nu,\nu')=\frac{\langle \delta I_{\mathrm{PL}}(\mathbf{r},\nu)\delta I_{\mathrm{PL}}(\mathbf{r},\nu')\rangle}{\langle I_{\mathrm{PL}}(\mathbf{r},\nu)\rangle\langle I_{\mathrm{PL}}(\mathbf{r},\nu')\rangle}, \tag{1}$$

where $\delta I_{\mathrm{PL}}(\mathbf{r},\nu)=I_{\mathrm{PL}}(\mathbf{r},\nu)-\langle I_{\mathrm{PL}}(\mathbf{r},\nu)\rangle$. The averaging $\langle\ldots\rangle$ is performed over the region of interest. Each element of the matrix $C_{\mathrm{PL}}(\nu,\nu')$ is an average of 8×10^3 correlated values. Normalization by the average PL intensities in Eq. (1) minimizes the influence of the intrinsic structure of QD emission spectrum (i.e., a spectrum that would be measured in the absence of disorder). Figure 2(a) shows the typical correlation matrix $C_{\mathrm{PL}}(\nu,\nu')$ for a sample with $k\ell^*=4$, where $k=(2\pi/\lambda)n_{\mathrm{eff}}$ is the effective wave number of light in the sample, n_{eff} is the effective refractive index, and ℓ^* is the transport mean free path [9]. We

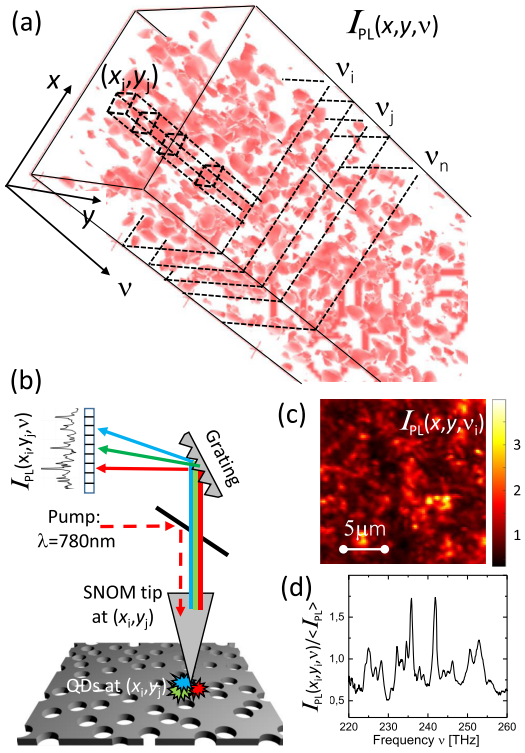

FIG. 1. Near-field hyperspectral imaging of QD photoluminescence. (a) Three-dimensional equi-intensity surface plot of PL signal $I_{\mathrm{PL}}(\mathbf{r},\nu)$ in a typical experimental scan. The total number of voxels of the three-dimensional image is of the order of 4×10^6. (b) Sketch of the experiment. (c) and (d) show PL intensity as a function of position for a given, randomly chosen frequency ν_i, and as a function of frequency for a given, randomly chosen position (x_i,y_i), respectively.

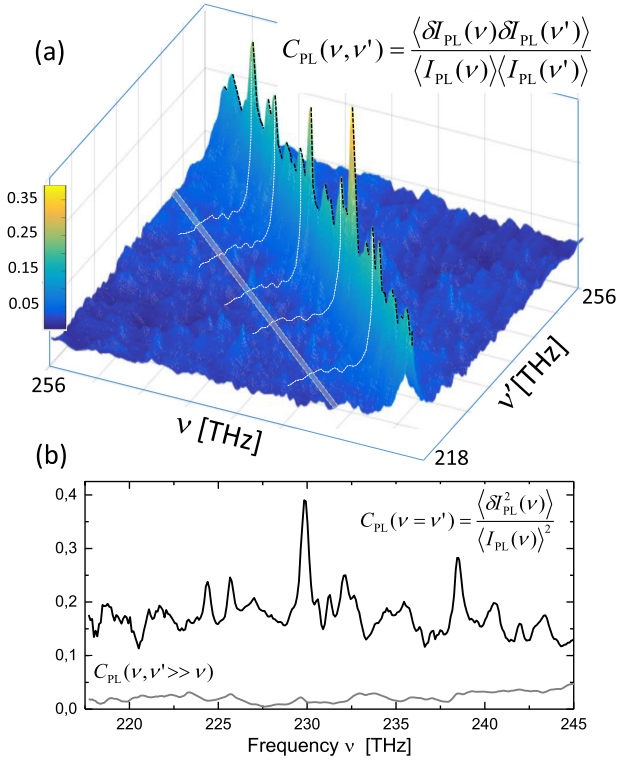

FIG. 2. Frequency-resolved correlation analysis. (a) Frequency correlation matrix of QD photoluminescence for a system with $k\ell^*=4$, which in terms of structural parameters corresponds to an average hole diameter $\langle d_h\rangle=210$ nm and a hole surface filling fraction $f=0.35$. (b) The diagonal elements of $C_{\mathrm{PL}}(\nu,\nu')$ equal to the normalized variance of PL intensity fluctuations (upper curve). The gray lower curve shows the fluctuations of off-diagonal terms ($\nu\neq\nu'$) at large detuning $\nu'\gg\nu$. It was evaluated along the gray line in the panel (a).

observe strong variations of $C_{\mathrm{PL}}(\nu,\nu')$ with frequencies. The variations are particularly pronounced for the diagonal elements $\nu=\nu'$ and are weaker for off-diagonal elements but persist even at large detunings $|\Delta\nu|=|\nu-\nu'|$. These variations are a combination of the intrinsic fluctuations of the system's parameters in space, residual statistical fluctuations due to a finite size of the statistical ensemble, and other extrinsic effects. The contribution of the latter is estimated to be below 20% of the overall signal variation [18]. The autocorrelation function $C_{\mathrm{PL}}(\Delta\nu)$ of the signal is obtained by averaging the correlation matrix over ν and ν' at a constant detuning $\Delta\nu$. This frequency averaging further decreases the contribution of extrinsic effects and allows for comparing experimental data $C_{\mathrm{PL}}(\Delta\nu)$ with theory.

In general, the relation between PL intensity due to QDs embedded in a disordered sample and radiative LDOS is not trivial. However, as discussed in Ref. [37] and further in Supplemental Material [18], for our samples, a linear relation can be established between PL intensity and the local density of states having the electric field component in the sample plane. For brevity, we abbreviate the latter quantity as LDOS in the following, although one has to understand that it represents only one of the contributions to the total LDOS. A linear relation between PL and LDOS accounts for roughly 80% of the measured signal [18]. Our calculation of the correlation function of LDOS integrated over a measurement area S, $\langle C_\rho(\Delta\nu)\rangle$, a quantity that can be directly compared to $C_{\mathrm{PL}}(\Delta\nu)$, is described in Supplemental Material [18]. The result is a sum of infinite-range (not decaying with $\Delta\nu$ as far as $|\Delta\nu|\ll\nu$) and short-range (rapidly decaying with $\Delta\nu$) contributions,

$$\langle C_\rho(\Delta\nu)\rangle = F_1(k\ell_\epsilon, ka, k\ell)\frac{\ln(2k\ell)}{\pi k\ell} + F_2(ka)\mathrm{Re}\left(\frac{D_B}{D(\Delta\nu)}-1\right), \quad (2)$$

where ℓ is the in-plane scattering mean free path [9]; a is the radius of the signal collection area S assumed circular. The renormalized in-plane diffusion coefficient $D(\Delta\nu)$ obeys [18,38]

$$\frac{D(\Delta\nu)}{D_B}=1-\frac{2}{\pi k\ell^*}\ln\left[1+\frac{D(\Delta\nu)\tau}{(s\ell^*)^2}\frac{1}{1-2\pi i\Delta\nu\tau}\right] \quad (3)$$

with $s \sim 1$, $D_B = (c/n_{\text{eff}})\ell^*/2$ being the Boltzmann diffusion coefficient, and τ the lifetime of a photon in our two-dimensional structure. The prefactors $F_{1,2} \leq 1$ in Eq. (2) account for the suppression of measured fluctuations due to the nonzero correlation length of fluctuations of the dielectric function ℓ_ϵ, and due to the nonzero size of signal collection area a.

The first term on the right-hand side of Eq. (2) is the so-called C_0 correlation function [39–41]. It is determined solely by the single scattering [42] near the measurement point; it does not depend on $\Delta\nu$ as long as $|\Delta\nu| \ll \nu$ and thus it is often referred to as "infinite range." Among all the possible scattering events, the single scattering is the fastest one and thus it determines the asymptotic behavior of $\langle C_\rho(\Delta\nu)\rangle$ at large detunings $\Delta\nu$. $\ln(2k\ell)/\pi k\ell$ in Eq. (2) represents LDOS variance for the white-noise disorder ($\ell_\epsilon \to 0$). The nonuniversal, disorder-specific nature of C_0 is encoded in the function F_1 that explicitly depends on the correlation length of disorder ℓ_ϵ and suppresses LDOS fluctuations with respect to their value for the white-noise disorder. The second term on the right-hand side of Eq. (2) is the multiple-scattering contribution to the correlation function decaying with $\Delta\nu$. This term is generated by photons that explore a large area on a time scale exceeding the mean free time ℓ/c. It encodes the information about multiple scattered photons and controls the decay of $\langle C_\rho(\Delta\nu)\rangle$ for small $\Delta\nu$. The function F_2 describes the suppression of this term due to the collection of signal from an area of nonzero size in the experiment. The size of the signal collection area a is the same for all our measurements. The suppression factor F_2 is evaluated analytically and it decreases with ka [18].

To fit the experimental data with Eq. (2) we consider the photon lifetime τ, the nonuniversal suppression factor F_1, and $s \sim 1$ as free fit parameters. ℓ, ℓ^*, and D_B are estimated using standard approaches from the number density of holes N, their average diameter $\langle d_h\rangle$, and the minimum distance D_{HC} between them [18]. These quantities can be measured with standard scanning electron microscopy (SEM) techniques taking advantage of the planarity of our samples.

Figure 3 shows examples of measured $C_{\text{PL}}(\Delta\nu)$ (black solid lines) compared with the theoretical $\langle C_\rho(\Delta\nu)\rangle$ (red dashed lines). The three curves correspond to three samples with different degrees of disorder, i.e., different values of $k\ell^*$ (samples A, B, and C, respectively, shown at the top of Fig. 3). The decay of $C_{\text{PL}}(\Delta\nu)$ with $\Delta\nu$ is well described by the second term in Eq. (2), whereas for large $\Delta\nu$, $C_{\text{PL}}(\Delta\nu)$ tends to a limit $C_{\text{PL}}(\infty) > 0$ equal to the first term. The amplitudes of both the short- and infinite-range contributions to $C_{\text{PL}}(\Delta\nu)$ decrease with $k\ell^*$, but the two contributions can be clearly separated in all cases.

Figure 4 shows the best-fit values of the nonuniversal prefactor F_1 plotted as a function of ℓ_ϵ and compared to a theoretical model in which the correlation function of disorder is assumed to have Gaussian shape [18]. Most

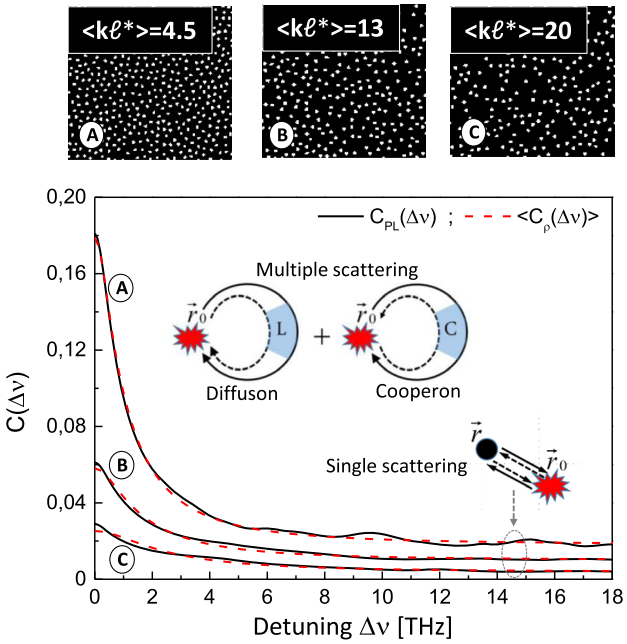

FIG. 3. Frequency correlation function of PL (black solid line) and the corresponding theoretical fit with $\langle C_\rho(\Delta\nu)\rangle$ (red dashed line) for samples with different scattering strengths $k\ell^*$. The inset shows scattering diagrams yielding different contributions to $\langle C_\rho(\Delta\nu)\rangle$. The classical (diffuson) and coherent (cooperon) diagrams are multiple scattering contributions that occur on large length and time scales and determine the behavior of $\langle C_\rho(\Delta\nu)\rangle$ at small detuning $\Delta\nu$ [18]. The single scattering is the fastest process that determines the asymptotic tail of $\langle C_\rho(\Delta\nu)\rangle$ at large $\Delta\nu$. The top of the image shows the SEM images of samples with different scattering strengths $k\ell^*$.

of the experimental data fall within the shaded area enclosed between lines corresponding to the two marginal values of ka for our set of samples.

The decay of $C_{\text{PL}}(\Delta\nu)$ is characterized by the lifetime τ of a photon inside the disordered system, or alternatively the Thouless frequency $\nu_{\text{TH}} = 1/\tau$ [9]. Figure 5(a) shows that the renormalized diffusion coefficient $D(\Delta\nu = 0)$ calculated using Eq. (3) with our best-fit values of τ and s, goes down to approximately 75% of its Boltzmann value D_B due to Anderson localization effects [43,44]. Localization effects are particularly strong in two-dimensional systems and originate from the interference between multiple scattered waves. They become more and more important as the strength of disorder increases, i.e., as $k\ell^*$ decreases, and they reduce the value of the diffusion coefficient that eventually goes to 0 in the limit of $k\ell^* \to 0$ or $\tau \to \infty$ [45]. The inset of Figure 5(a) shows the best-fit values of $3D_B\tau/\ell^{*2}$ for our set of samples. This parameter roughly corresponds to the number of scattering events experienced by a photon before leaving the sample. The blue shaded area in Fig. 5(a) is enclosed between the curves corresponding to the two marginal values of $3D_B\tau/\ell^{*2}$. Losses of energy resulting in a finite lifetime τ of a photon

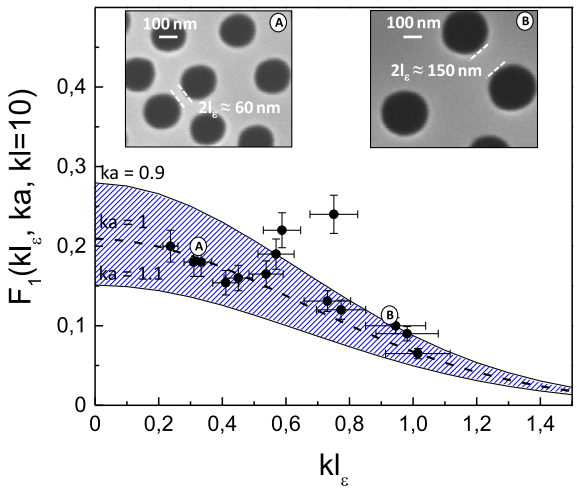

FIG. 4. Values of F_1 (black points) obtained from the fits to the measured $C_{\mathrm{PL}}(\Delta\nu)$ by Eq. (2). The two continuous lines and the dashed line show the behavior of F_1 expected from the theory for $ka = 0.9$, 1.1, and 1, respectively, and for $k\ell = 10$ that is typical for the whole set of samples (the dependence on $k\ell$ is very weak). The two insets show the sensitivity of F_1 to the average minimum distance between adjacent scatterers $2\ell_\epsilon$ [18].

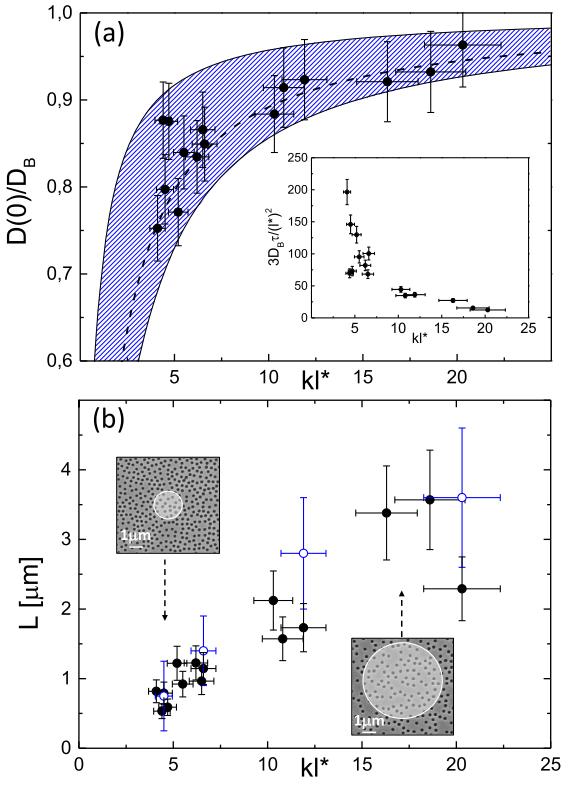

FIG. 5. (a) Renormalization of the diffusion constant $D(0)$ as a function of $k\ell^*$. Full black circles are the values obtained from the theoretical fits to the measured autocorrelation function of PL. The two solid lines show the marginal values of $D(0)/D_B$ for our set of samples. The inset shows the values of the dimensionless parameter $3D_B\tau/\ell^{*2}$ that roughly corresponds to the number of scattering events experienced by a photon before leaving the sample. (b) Characteristic length scale L as a function of $k\ell^*$. The four empty circles are the direct measurements of the decay length of photonic modes taken from Ref. [17]. The two insets show the schematic representation of L for two values of $k\ell^*$. L shrinks with decreasing $k\ell^*$.

make the two-dimensional material behave as if it was of finite extent $L \sim \sqrt{D_B\tau}/s$. The length scale L encodes the in-plane scattering properties via D_B and the total loss time τ of the real three-dimensional system. The latter is mainly due to out-of-plane leakage but also accounts for in-plane losses due to the finite sample size. Figure 5(b) shows that L increases with $k\ell^*$ (full black circles); its values are similar to the values of the spatial decay length of photonic modes directly measured in Ref. [17] [empty blue circles in Fig. 5(b)]. For an infinite two-dimensional disordered system without loss, the latter quantity would be equal to the localization length ξ [46]. A separation between contributions of localization and loss to the decay rate of modes in a realistic experiment can be realized by analyzing the statistics of their quality factors [47].

The results of our experiments can be summarized as follows. A QD emits light at a given position $\mathbf{r}$ inside the disordered material and the intensity of emission is measured at the same position $\mathbf{r}$. The single scattering is the fastest mechanism that produces fluctuations of the measured signal with $\mathbf{r}$. This fast contribution gives rise to a large-$\Delta\nu$ tail of $C_{\mathrm{PL}}(\Delta\nu)$. Structural correlations of disorder decrease the amplitude of the signal with respect to its value for uncorrelated (white-noise) disorder but the signal remains well above the noise level and is easily detectable. On the other hand, multiple scattering occurs on longer time scales. It samples a macroscopically large portion of material and has a strong frequency dependence. This mechanism determines the decay of $C_{\mathrm{PL}}(\Delta\nu)$ towards the asymptotic value determined by the single scattering. Partial averaging of PL fluctuations over the measurement area S reduces both single- and multiple-scattering parts of $C_{\mathrm{PL}}(\Delta\nu)$.

In conclusion, in this work we clearly separate the infinite- and the short-range contributions to the frequency correlation function $C_{\mathrm{PL}}(\Delta\nu)$ of QD photoluminescence. The latter describes the decay of $C_{\mathrm{PL}}(\Delta\nu)$ with $\Delta\nu$ whereas the former accounts for its asymptotic value at large $\Delta\nu$. A direct link between $C_{\mathrm{PL}}(\Delta\nu)$ and the correlation function of LDOS $\langle C_\rho(\Delta\nu)\rangle$ is established. Both contributions to $C_{\mathrm{PL}}(\Delta\nu)$ can be understood in the framework of our theoretical model showing that the infinite-range part of $C_{\mathrm{PL}}(\Delta\nu)$ explicitly depends on the disorder correlation length whereas its short-range part is mainly controlled by the renormalization of diffusion due to Anderson localization effects. The separation of physical phenomena behind the two contributions to $C_{\mathrm{PL}}(\Delta\nu)$ and hence to $\langle C_\rho(\Delta\nu)\rangle$ allows for efficiently designing a disordered material featuring a particular shape of $\langle C_\rho(\Delta\nu)\rangle$. These results pave a way towards designing disordered photonic materials with desired LDOS statistics, opening new

perspectives for light-harvesting [1,2], quantum-optics [3], and light-emission [4] applications of disordered materials.

F. R. acknowledges P. Sebbah for his help at the initial stage of data analysis, A. Fiore and A. Gerardino for sample fabrication, and K. Vynck, S. Vignolini, F. Sgrignuoli, and D. S. Wiersma for many fruitful discussions. F. R. acknowledges financial support from the University of Trento Starting Grant Young Researchers Grant No. 40600009. S. E. S. acknowledges financial support from the Agence Nationale de la Recherche Grant No. ANR-14-CE26-0032 LOVE.

*francesco.riboli@ino.it
†Sergey.Skipetrov@lpmmc.cnrs.fr

[1] A. Polman and H. A. Atwater, Nat. Mater. **11**, 174 (2012).
[2] K. Vynck, M. Burresi, F. Riboli, and D. S. Wiersma, Nat. Mater. **11**, 1017 (2012).
[3] L. Sapienza, H. Thyrrestrup, S. Stobbe, P. D. García, S. Smolka, and P. Lodahl, Science **327**, 1352 (2010).
[4] D. S. Wiersma, Nat. Phys. **4**, 359 (2008).
[5] B. Redding, M. A. Choma, and H. Cao, Nat. Photonics **6**, 355 (2012).
[6] B. Redding, S. F. Liew, R. Sarma, and H. Cao, Nat. Photonics **7**, 746 (2013).
[7] R. Pappu, B. Recht, J. Taylor, and N. Gershenfeld, Science **297**, 2026 (2002).
[8] S. A. Goorden, M. Horstmann, A. P. Mosk, B. Skoric, and P. W. H. Pinkse, Optica **1**, 421 (2014).
[9] E. Akkermans and G. Montambaux, *Mesoscopic Physics of Electrons and Photons* (Cambridge University Press, Cambridge, 2007).
[10] R. G. S. El-Dardiry, S. Faez, and A. Lagendijk, Phys. Rev. A **83**, 031801(R) (2011).
[11] R. Loudon, *The Quantum Theory of Light* (Oxford University Press, Oxford, 1983).
[12] M. D. Birowosuto, S. E. Skipetrov, W. L. Vos, and A. P. Mosk, Phys. Rev. Lett. **105**, 013904 (2010).
[13] V. Krachmalnicoff, E. Castanié, Y. De Wilde, and R. Carminati, Phys. Rev. Lett. **105**, 183901 (2010).
[14] R. Sapienza, P. Bondareff, R. Pierrat, B. Habert, R. Carminati, and N. F. van Hulst, Phys. Rev. Lett. **106**, 163902 (2011).
[15] P. D. García, S. Stobbe, I. Söllner, and P. Lodahl, Phys. Rev. Lett. **109**, 253902 (2012).
[16] B. A. van Tiggelen and S. E. Skipetrov, Phys. Rev. E **73**, 045601 (2006).
[17] F. Riboli, N. Caselli, S. Vignolini, F. Intonti, K. Vynck, P. Barthelemy, A. Gerardino, L. Balet, H. L. Li, A. Fiore, M. Gurioli, and D. S. Wiersma, Nat. Mater. **13**, 720 (2014).
[18] See Supplemental Material http://link.aps.org/supplemental/10.1103/PhysRevLett.119.043902 for additional details of experimental procedures and a derivation of the theoretical model, which includes Refs. [19–36].
[19] Q. Wang, S. Stobbe, and P. Lodahl, Phys. Rev. Lett. **107**, 167404 (2011).
[20] R. Sapienza, T. Coenen, J. Renger, M. Kuttge, N. F. van Hulst, and A. Polman, Nat. Mater. **11**, 781 (2012).
[21] G. Colas des Francs, C. Girard, J. Weeber, and A. Dereux, Chem. Phys. Lett. **345**, 512 (2001).
[22] S. Vignolini, F. Intonti, F. Riboli, D. S. Wiersma. L. Balet. L. H. Li, M. Francardi, A. Gerardino, A. Fiore, and M. Gurioli, Appl. Phys. Lett. **94**, 163102 (2009).
[23] J. Wenger, D. Gerard, J. Dintinger, O. Mahboub, N. Bonod, E. Popov, T. W. Ebbesen, and H. Rigneault, Opt. Express **16**, 3008 (2008).
[24] A. F. Koenderink, M. Kafesaki, B. C. Buchler, and V. Sandoghdar, Phys. Rev. Lett. **95**, 153904 (2005).
[25] K. Joulain, R. Carminati, J. P. Mulet, and J. J. Greffet, Phys. Rev. B **68**, 245405 (2003).
[26] Y. De Wilde, F. Formanek, R. Carminati, B. Gralak, P. A. Lemoine, K. Joulain, J. P. Mulet, Y. Chen, and J. J. Greffet, Nature (London) **444**, 740 (2006).
[27] M. Gurioli, A. Vinattieri, M. Zamfirescu, and M. Colocci, S. Sanguinetti, and R. Nötzel, Phys. Rev. B **73**, 085302 (2006).
[28] N. Caselli, F. Riboli, F. Intonti, F. La China, F. Biccari, A. Gerardino, and M. Gurioli, APL Photonics **1**, 041301 (2016).
[29] S. Stobbe, J. Johansen, P. T. Kristensen, J. M. Hvam, and P. Lodahl, Phys. Rev. B **80**, 155307 (2009).
[30] C. F. Wang, A. Badolato, I. Wilson-Rae, P. M. Petroff, E. Hu, J. Urayama, and A. Imamoglu, Appl. Phys. Lett. **85**, 3423 (2004).
[31] X. W. Chen, V. Sandoghdar, and M. Agio, Phys. Rev. Lett. **110**, 153605 (2013).
[32] N. Caselli, F. Intonti, F. La China, F. Riboli, A. Gerardino, W. Bao, A. Weber Bargioni, L. Li, E. H. Linfield, F. Pagliano, A. Fiore, and M. Gurioli, Light Sci. Appl. **4**, e326 (2015).
[33] L. Novotny and B. Hecht, *Principles of Nano-Optics* (Cambridge University Press, New York, 2007).
[34] D. Vollhardt and P. Wölfle, in *Electronic Phase Transitions* (Elsevier Science, Amsterdam, 1992), p. 1.
[35] N. Cherroret and S. E. Skipetrov, Phys. Rev. E **77**, 046608 (2008).
[36] G. M. Conley, M. Burresi, F. Pratesi, K. Vynck, and D. S. Wiersma, Phys. Rev. Lett. **112**, 143901 (2014).
[37] F. Intonti, S. Vignolini, F. Riboli, A. Vinattieri, D. S. Wiersma, M. Colocci, L. Balet, C. Monat, C. Zinoni, L. H. Li, R. Houdré, M. Francardi, A. Gerardino, A. Fiore, and M. Gurioli, Phys. Rev. B **78**, 041401(R) (2008).
[38] L. P. Gor'kov, A. I. Larkin, and D. E. Khmel'nitskii, JETP Lett. **30**, 228 (1979).
[39] B. Shapiro, Phys. Rev. Lett. **83**, 4733 (1999).
[40] S. E. Skipetrov and R. Maynard, Phys. Rev. B **62**, 886 (2000).
[41] W. K. Hildebrand, A. Strybulevych, S. E. Skipetrov, B. A. van Tiggelen, and J. H. Page, Phys. Rev. Lett. **112**, 073902 (2014).
[42] We use the term single scattering for brevity. In reality, light may be multiply scattered but only a single common scattering event is allowed between two waves returning to the source point (see the inset of Fig. 3). This effectively restricts the relevant area around the source to $\sim \ell^2$.
[43] P. W. Anderson, Phys. Rev. **109**, 1492 (1958).

[44] *50 Years of Anderson Localization*, edited by E. Abrahams (World Scientific, Singapore, 2010).
[45] E. Abrahams, P. W. Anderson, D. C. Licciardello, and T. V. Ramakrishnan, Phys. Rev. Lett. **42**, 673 (1979).
[46] D. Laurent, O. Legrand, P. Sebbah, C. Vanneste, and F. Mortessagne, Phys. Rev. Lett. **99**, 253902 (2007).
[47] S. Smolka, H. Thyrrestrup, L. Sapienza, T. B. Lehmann, K. R. Rix, L. S. Froufe-Pérez, P. D. García, and P. Lodahl, New J. Phys. **13**, 063044 (2011).